Shear resistance of headed shear studs welded on welded plates in composite floors

T. Molkens[1], Jelena Dobrić[3], Barbara Rossi[1,2]

[1] KU Leuven, Department of Civil Engineering, tom.molkens@kuleuven.be, barbara.rossi@kuleuven.be (corresponding author)

[2]University of Oxford, Department of Engineering Science, Barbara.rossi@new.ox.ac.uk

[3]University of Belgrade, Faculty of Civil Engineering, jelena@imk.grf.bg.ac.rs

Abstract

The present paper deals with composite steel-concrete floor with headed shear studs welded onto a flat steel plate. In some wide slab applications, the most performant lay-out for the studs could lead to a possible option in which the studs are welded on top of an existing butt weld between steel plates. Presently, the shear resistance of the weld to weld interface and its possible detrimental effect on the overall resistance of the system is studied. Two types of tests were performed: pure shear tests complying to the push-out tests to Annex B of EN 1994-1-1 and beam tests with four-point loading where the studs in the shear spans are loaded with longitudinal shear. For each pair of tests, the reference specimen was made with a steel plate without a butt weld and the actual specimen comprising a butt weld in the plate directly in the position where the stud is connected. No difference in shear capacity, stiffness or failure mode could be observed. However, it was noticed that the classic design rules provided in EN1994-1-1 cannot accurately predict the failure load of the chosen configuration. In fact, the present paper deals with thick steel plates combined with a relatively moderate layer of concrete, specific for bridges applications. The ultimate behaviour of the system is combining the flexural resistance of a composite cross-section followed by, when the concrete is cracked, the development of a compressed arch anchored in the headed shear studs underlying the importance of such connections. An in-depth analysis on the behaviour of the system at ultimate limit state is proposed.

Keywords: Push-out test, four-point bending tests, longitudinal shear resistance, composite floor, butt weld

TABLE OF CONTENTS

List of symbols

a	Distance between the support and the point load in the four-point bending tests	[mm]
A_s	Cross-sectional area of the reinforcement	[mm²]
b	Mean width of the steel plate	[mm]
b_c	Mean width of the concrete slab	[mm]
$C_{Rd,c}$	Calibration factor for the shear capacity of members without shear reinforcement	/
d	Diameter of the shank of the stud or distance from the top of the concrete to the centroid of the reinforcement bars	[mm]
d_{conc}	Distance from extreme compressed concrete fibre to centroid of the reinforcement	[mm]
E_a	Modulus of elasticity of the steel	[N/mm²]
E_s	Modulus of elasticity of the steel reinforcement	[N/mm²]
E_{cm}	Modulus of elasticity of the concrete	[N/mm²]
f_{ck}	Characteristic cylinder compressive strength of the concrete	[N/mm²]
$f_{cm,\ 28days}$	Mean cylinder compressive strength of the concrete after 28 days	[N/mm²]
$f_{cm,\ test}$	Mean cylinder compressive strength of the concrete on the day of the test	[N/mm²]
$f_{u,\ plate}$	Ultimate strength of the steel plate	[N/mm²]
$f_{u,\ stud}$	Ultimate strength of the stud	[N/mm²]
$f_{y,\ plate}$	Yield strength of the steel plate	[N/mm²]
$f_{y,\ stud}$	Yield strength of the stud	[N/mm²]
h_c	Mean thickness of the concrete slab	[mm]
h_{sc}	Overall height of the stud	[mm]
k	size factor valid for shear capacity	/
L	Span or distance between load	[mm]
n	Number of studs	/
P	Total load in the push-out test or in the four-point bending test	[kN]
$P_{f,\ total}$	Total failure load	[kN]
P_{max}	Maximum force	[kN]

$P_{Rd,\ stud}$	Design value of the shear resistance of a single connector	[kN]
P_{Rk}	Characteristic value of the shear resistance of a single connector	[kN]
t	Thickness steel plate	[mm]
x	Thickness of the uncracked concrete layer	[mm]
z	Position of the centroid of the cross-section	[mm]
α	Parameter in the resistance formula for the stud	/
Δ	Deflection	[mm]
δ_u	Maximum slip measured at P_{Rk}	[mm]
δ_{uk}	Characteristic value of slip capacity	[mm]
η	Degree of the shear connection	/
γ	Partial safety factor	/
ρ_l	Reinforcement ratio of longitudinal reinforcement	/

1 INTRODUCTION AND STATE OF THE ART

Composite members are widely used in constructions, combining the favourable properties of different materials to create optimized construction parts. The combination of steel and concrete in beams and floors is one of the most well-known examples. The shear connection is realized by using mechanical shear connectors which can have a variety of shapes. Headed shear studs are the most widely used solution in composite construction. The present paper deals with headed shear studs welded onto a flat steel plate, as displayed in Figure 1(a) with some typical dimensions.

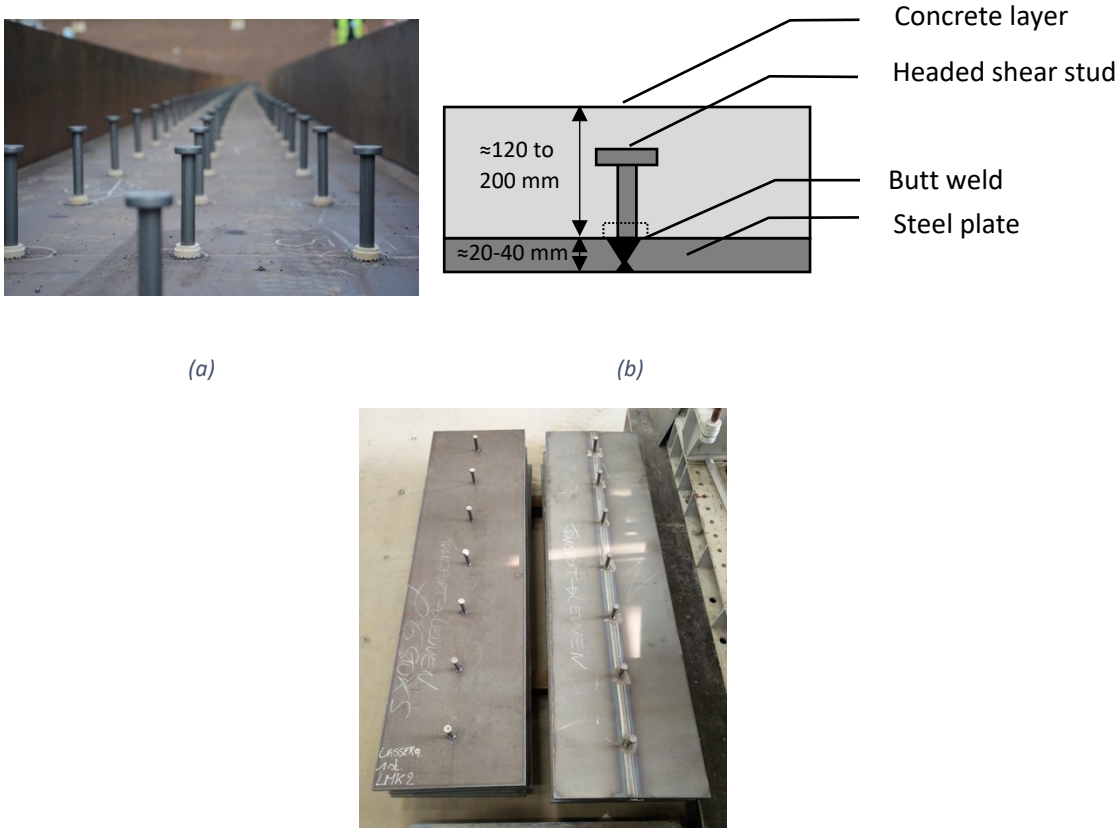

Figure 1: Shear studs in place before welding (Anon., sd) (a), scheme of the studied system (b) and specimens for four-point bending test before concreting (left: unwelded, right: welded)

Depending on constructive detailing, optimal placement of the studs and/or limited available space may require the studs to be positioned right on top of an existing butt weld (Figure 1(b)). Despite the large amount of information available in the literature on the behaviour of shear studs, very little is known about the effect of welding a stud on a butt weld although this might have a detrimental effect on the shear resistance of the weld to weld interface. One of the objectives of this research is to investigate the effect on the shear resistance of the studs when there is a butt weld directly in the location where the studs are welded on the steel plate.

In addition, the present paper deals with thick steel plates combined with a concrete layer of limited thickness which is often encountered in bridges applications. According to the current design methods, the vertical shear capacity of composite beams equals the shear capacity of the steel section, except if the concrete contribution can be established. Instead, for composite floor made with corrugated thin-walled steel sheets, the concrete contribution only is influencing the capacity of the composite

system. For now, there is no rule when thick steel plates are used in combination with a relatively thick layer of concrete like in bridge decks. However, in between stiffeners due to local bending (for example coming from an axle load), this is a common situation. An additional verification should be carried out to detect the possibility of premature failure due to a lack in vertical shear capacity of the concrete layer. Additionally, as it will be highlighted herein, the behaviour of the system is combining the flexural resistance of a composite cross-section followed by, when the concrete is cracked, the development of a compressed arch anchored in the headed shear studs underlying the importance of such connections. Without such verification there is a risk that due to local loads, the steel plate bellow the concrete topping could fail and creates in the global system even a hinge, where this is not the meaning.

A concise literature survey below is provided focusing on how the shear resistance of headed studs has been tested in the references of experimental research.

In (An & Cederwall, 1996), the influence of high strength concrete and/or reinforcement on the shear capacity of the studs was investigated. Therefore, samples were made combining either normal or high strength concrete with one or two layers of reinforcement mesh, see Figure 2. The load was cycled 25 times between 5% and 40% of the expected failure load. Traditional push-out tests as well as tensile tests on studs, compression tests on concrete cylinders and cubes and concrete splitting tests to measure the tensile strength of the concrete were carried out. The longitudinal slip between the steel profile and the concrete slabs, the separation of the slabs from the profile and the strain on the reinforcement bar via strain gauges were measured.

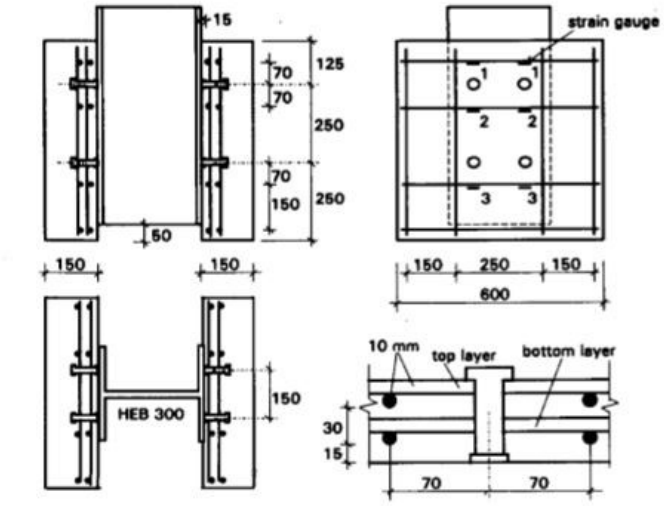

Figure 2: Push-out test (An & Cederwall, 1996)

In (Qi, et al., 2017), the effect of initial damage on the shear capacity of the stud was investigated. The same testing set-up as in (An & Cederwall, 1996) was used with varying degrees of initial damages. In (Kumar, et al., 2017), a hot-rolled UC profile was connected to concrete slabs using a single shear stud. The slabs were casted in a vertical position, using a steel formwork. This type of specimen was used for both push-out tests and impact tests. To perform the impact tests, a 4,5 kg steel ball was repeatedly dropped through a steel pipe onto the steel profile. In (Alkhatib, 2012), again the specimens consist of a steel W250x28 profile connected to thick concrete slabs by shear studs (two instead of one) varying in their types and sizes. The slabs were casted in a vertical position, using a plywood formwork securing the steel section firmly.

In (Easterling, et al., 1993), push-out tests were conducted on composite floor specimens where the studs were welded on a corrugated steel sheet used as formwork for the concrete slab. The specimen was made in two halves, each consisting of a steel WT-profile with a profiled sheet and a concrete slab on top, Figure 3. The studs were welded through the sheet onto the profile. The two halves allow the concrete to be poured horizontally, and from the same concrete mix. When the concrete has cured, the two T-profiles were bolted together.

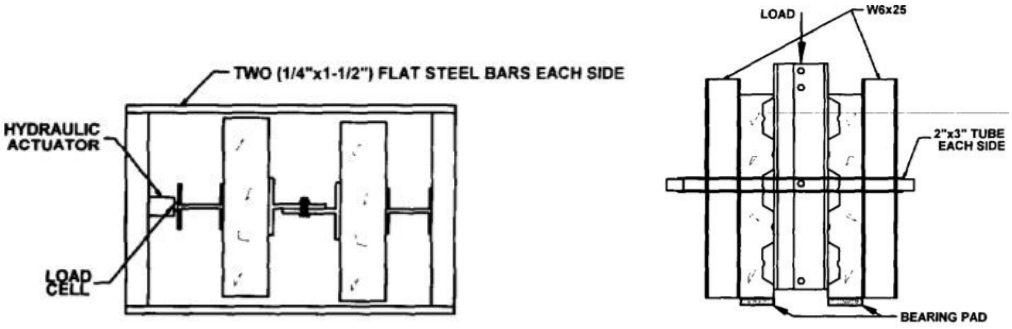

*Figure 3: Push-out setup (Easterling, et al., 1993) **&** (Cashell & Baddoo, 2013)*

In (Cashell & Baddoo, 2013), the specimens are based on the standard push-out test as prescribed in (EN1994-1-1, 2004). However, the hot-rolled steel profile was again replaced by 2 steel T-profiles bolted together as in (Easterling, et al., 1993). This allows both concrete slabs to be cast at the same time, using the same concrete mix. In accordance with (EN1994-1-1, 2004), the load was cycled 25 times between 5% and 40% of the expected failure load. In (Horita, et al., 2012), the setup was designed to test the behaviour of studs with a large diameter in shear. The slabs were connected to a steel T-profile by 1, 2 or 3 stud(s) and, as previously, the webs of the T-profiles were bolted together to create I-profile section. Along with a pair of vertical supports placed underneath the concrete slabs, lateral restraints were installed to avoid any horizontal movement of the slabs, Figure 4. This was done to prevent any rotational deformation occurring in the steel deck.

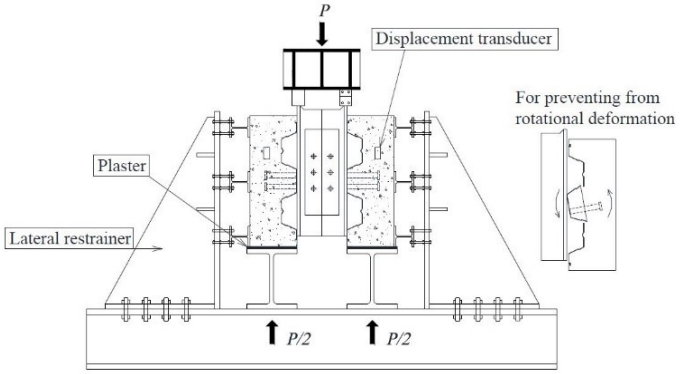

Figure 4: Push-out setup (Horita, et al., 2012)

In (Prakash, et al., 2012), the studs used in the experimental programme were made of high strength steel. As a consequence of the 900 MPa ultimate strength of the studs, the number of studs was decreased from 4 to 2 per slab and placed in a single layer. Apart from the decreased number of studs, there were 2 major differences between these tests and the standard test as prescribed in (EN1994-1-1, 2004):

- The concrete slabs are designed considering the confinement effect of the concrete, allowing the specimens to be narrower (300 mm compared to the 600 mm wide slabs in the standard test).

- The second major difference is the casting of the concrete. According to (EN1994-1-1, 2004), both slabs should be casted in a horizontal position, as it would be done in practice. In this case however, the slabs were casted in a vertical position.

The concrete slabs were confined at the bottom using tie rods with a diameter of 16 mm.

In (Wang, et al., 2011), the shear capacity of large studs with diameters ranging from 22 to 30 mm, combined with a varying strength of the stud was studied. The used setup was a modified push-out test with very stocky concrete blocks. As was done in (Easterling, et al., 1993), the steel profile was bolted together after the casting of the concrete, allowing for both sides to be casted from the same batch. One out of three specimens is tested under cyclic loading, the others under monotonic loading.

In (Shim, et al., 2010), the push-out specimens were made using high-strength concrete slabs. The width and thickness of the slabs was significantly larger than those of the standard push-out test, as described in (EN1994-1-1, 2004). The concrete was poured via a 510 m pipe, in order to simulate the conditions of a high-rise construction. Additional studs were used to connect the concrete slabs to the base plate of the specimen.

In (Lowe, et al., 2014), a completely new setup was developed to investigate the behaviour of a composite beam when the concrete fails by splitting along the line of the studs. Via a loading jack, a horizontal load was imposed along one steel profile onto which the concrete beam was casted. The concrete part of the composite specimen was horizontally supported by a reaction wall, Figure 5. Five tests were conducted. Four of these were tested using a monotonic loading procedure, the fifth one using a cyclic loading procedure with 25 cycles.

The global slip was measured, as well as local slip at the level of each stud. Furthermore, portal gauge wire ran through the concrete on 22 locations to measure the outward displacement of both sides of the concrete rib.

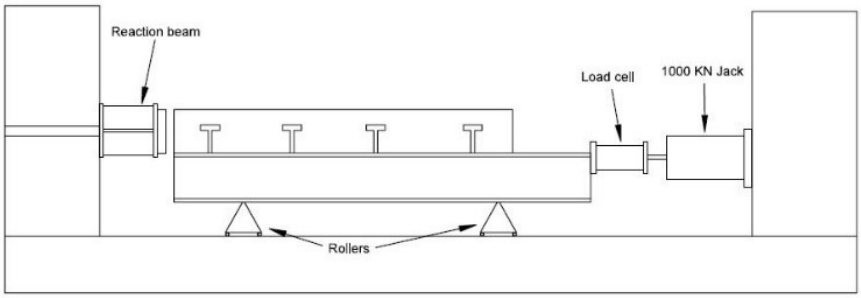

Figure 5: Push rig setup

In (Rehman, et al., 2018), four-point bending tests were carried out on slabs consists consisting of a steel IPE300-profile on top of which a steel deck was placed. Before the concrete slab was casted, either demountable or welded shear studs were connected to the plate.

2 TYPE OF TEST, SAMPLES GEOMETRY AND SET UP

All specimens were prepared according to annex B of (EN1994-1-1, 2004). The tests were designed to evaluate the shear resistance of 19 mm headed studs (h_{sc} = 100 mm) welded onto a steel plate of a thickness t =30mm in which a butt weld already exist (d/t = 0.63). The butt weld was realised following LMB C558 under powder – process 121 and the studs were welded on that weld following LMB H505 stud welding with ceramic ring – process 783. The manufacturer provided the mechanical

characteristics of one representative sample of the shear connector material as well as of the thick steel plate onto which those connectors were welded, see Table 1. The shear connectors and steel plates were taken from the same batch. The obtained plate together with its reinforced concrete layer is typically used in bridge applications. The samples are denoted PO for push-out, W for welded, NW for non-welded, PL for non-welded plates and WE for welded plates.

Table 1: Mechanical properties of the plate and studs as provided by the manufacturer

	$f_{y,\,plate}$ [N/mm²]	$f_{u,\,plate}$ [N/mm²]	$f_{y,\,stud}$ [N/mm²]	$f_{u,\,stud}$ [N/mm²]
Steel properties	460	540	511	527

2.1 PUSH-OUT TEST

2.1.1 Dimensions and set up

Figure 6 shows the nominal dimensions of the push-out samples that were presently tested. Three of these samples were made. In two of these, the shear studs were welded on a butt weld. To enable this butt weld to be performed, a box profile was chosen instead of the HEB 260 as prescribed in (EN1994-1-1, 2004). The dimensions of the concrete slabs were chosen to be as close as possible to the standard specimen, while meeting all the criteria set in (EN1994-1-1, 2004) Annex B, with minimum reinforcement. The slabs were casted in the horizontal position, as is done for composite beams in practice. The tests are displacement based with a loading rate ranging between 71 and 80 N/s.

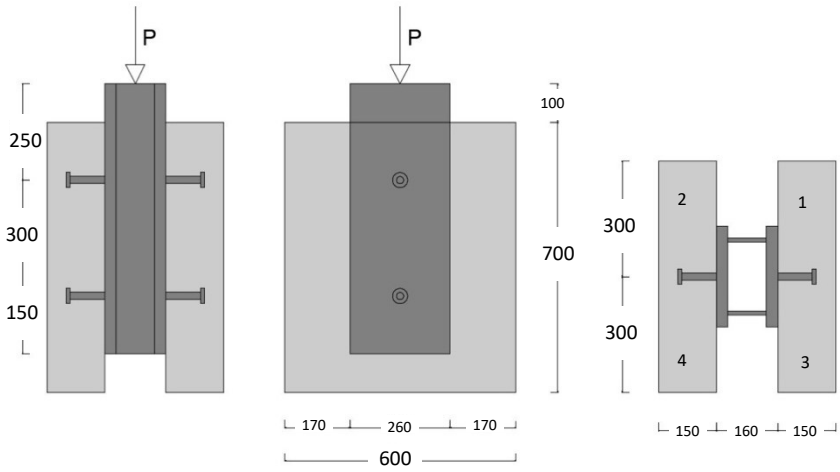

Figure 6: Push-out specimen and positions of the LVDT's (1, 2, 3 and 4)

For the push-out tests, the specimens were concreted with one mixer using the same recipe. For each test, six concrete cubes (150 x 150 x 150 mm) were made to determine the compressive strength of the concrete. Three of the cubes were cured in the same place as the specimen. The other three cubes were cured in a climatized room with a constant temperature of 20°C and air humidity above 90% according to EN 12390-1:2000. Before the cubes were tested, they were carefully measured. The cubes cured in the climatized room were used to determine the compressive strength of the concrete after 28 days. The other three cubes were tested on the same day as the specimen itself. The average compressive strength $f_{cm,28days}$ is 57,6MPa or 50,8MPa for the PO-NW and the PO-W specimens respectively and the average compressive strength $f_{cm,test}$ is 63,3MPa or 55,9MPa for the PO-NW and the PO-W specimens respectively. The effective dimensions of the steel plate and concrete layer as

well as position of each stud were also carefully measured for each specimen as were the angles of the stud with the steel plate. The angles of the stud with the steel plate were measured, it equals 90,3° on average with a standard deviation of 1,7° i.e. practically vertical.

The test setup, Figure 7, for the push-out tests was developed according to (EN1994-1-1, 2004) annex B. Steel plates are always treated with formwork oil to eliminate bond at the interface with the concrete.

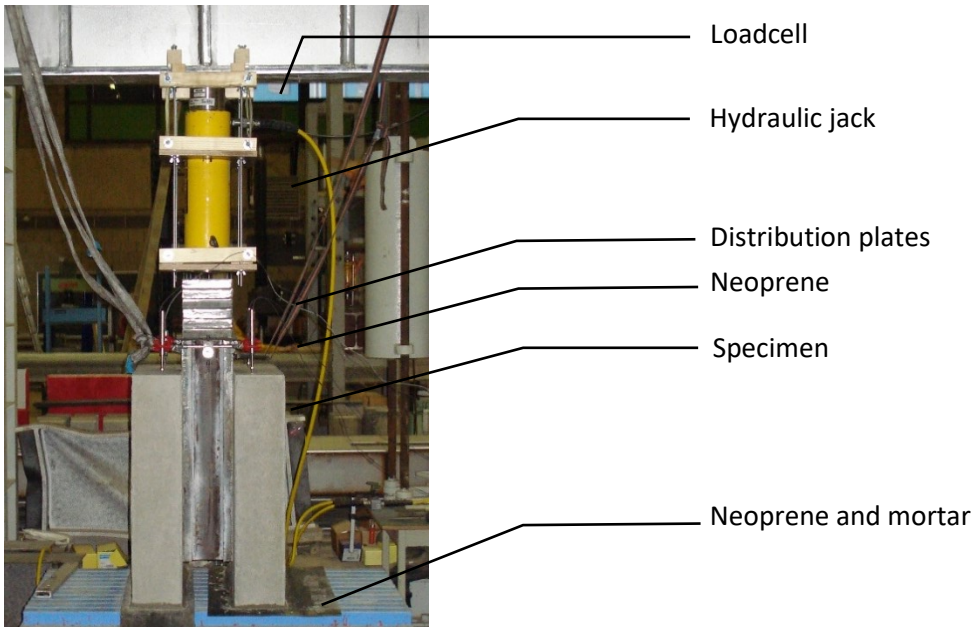

Figure 7: push-out setup

The steel box profile which was designed for this test consists of 4 steel plates welded together. For this reason, the top surface was not completely horizontal. To even out the imperfections, a piece of neoprene was placed between the box profile and the steel distribution plates. The bottom surface of the concrete slabs of each specimen were also never completely straight and parallel to each other. To level the imperfections and prevent concentration of stresses, a layer of high resisting mortar together with a layer of neoprene were placed in-between the specimen and the supporting concrete block.

2.1.2 Actuators

For the push-out and bending test respectively, one or two actuators Enerpac RC-7513 with a maximum capacity of 718 kN were used to generate the load. The force was measured using a loadcell, placed between the hydraulic jack and the test frame, with a maximum capacity of 800 kN.

2.1.3 Displacements

Four displacement transducers (Linear Variable Differential Transducer, LVDT) were used to measure the relative longitudinal slip between the concrete slabs and the steel profile. The LVDT's used for these tests have a maximum stroke length of 20 mm. The LVDT's were placed on top of each specimen as depicted in Figure 6 (positions 1, 2, 3 and 4).

Two threaded rods (Figure 8) were placed through the steel box section. On each rod, 2 clamps (in red) were used to position the LVDT's.

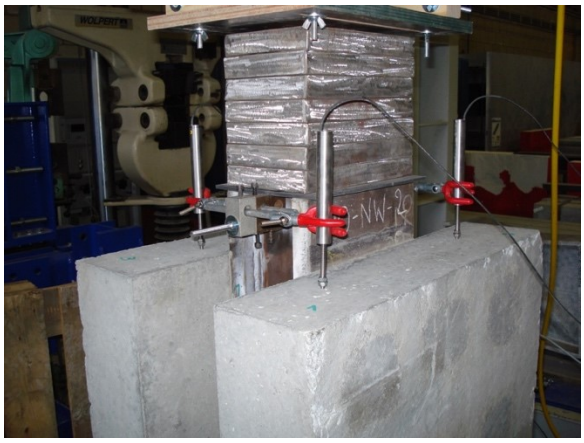

Figure 8: Threaded rod and LVDT's

2.1.4 Testing procedure

The testing procedure for the push-out tests is described in annex B of (EN1994-1-1, 2004). In the prescribed testing procedure, the measuring devices should continuously measure the slip until the load has dropped under 20% of the maximum load. Before this the LVDT's were removed to protect them from being damaged when the specimen fails. The load was increased in steps up to 40% of the expected failure load and then 25 cycles between 5% and 40% of the expected failure load were carried out. After this, the load was increased up until failure.

EN 1994-1-1 does not specify any exact duration time for the test, except that after the initial load cycling the failure should not occur in less than 15 minutes.

2.2 FOUR-POINT BENDING TEST

2.2.1 Dimensions and set up

Figure 9 presents the nominal dimensions of the specimens in the four-point bending test, where a longitudinal butt weld runs along the length of the entire plate in the centreline of the plate cross-section. The studs are welded on top of the butt weld. The tests are also displacement based with a loading rate ranging between 30 and 40 N/s in the first phase and 15 to 20 N/s when concrete is cracked.

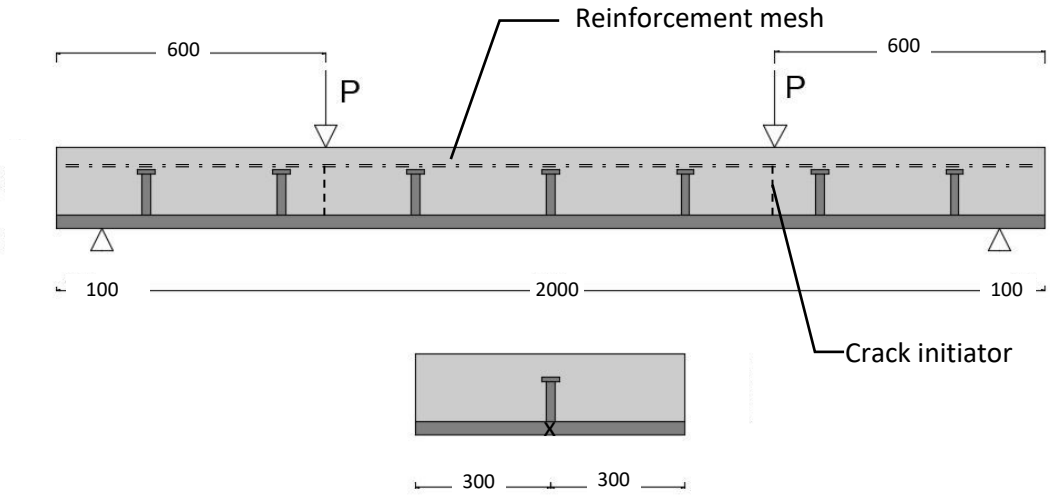

Figure 9: four-point bending test specimen

Two crack initiators of 110mm were located on the steel plate (dashed line in Figure 9), on top of which four rebars of 8 mm BE500 were placed (in the longitudinal direction, Figure 9) with an interspace of 150 mm. Transverse bars of the same diameter and interspace were also used. To evaluate the theoretical resistance correctly, the effective dimensions of the steel plate and concrete layer, see Table 2, were carefully measured for each specimen. Out of this table it can be seen that on top of the crack initiators, a continuous compression layer of at least 50 mm is at our disposal.

Table 2: Effective dimensions of the specimens [mm]

	WE-1	**PL-2**
Mean width of the steel plate b	599,2	599,9
Mean steel thickness t	30,7	30,9
Mean concrete width b_c	595,0	595,6
Mean concrete thickness h_c	163,9	164,2

For the four-point bending tests, the specimens were concreted using two mixers using the same recipe. Four cubes (150 x 150 x 150 mm) were made for each mixer. Two cubes were cured in the same place as the specimen and two cubes were cured in a climatized room at 20°C and an air humidity of at least 90% to determine the compressive strength after 28 days. The cubes cured in the same place as the specimen, are tested the same day as the floor slice, as was done for the push-out tests. All the cubes were measured with an accuracy of 0,01 mm before testing. The average compressive strength $f_{cm,28days}$ is 53,2 MPa or 58,1 MPa for the PL and the WE specimens respectively and the average compressive strength $f_{cm,test}$ is 56,9 MPa or 61,0 MPa for the PL and the WE specimens respectively.

The test setup was built according to (EN1994-1-1, 2004) annex B. To limit the slip between the concrete layer and the steel plate, a minimum degree of shear connection is needed. In (EN1994-1-1, 2004), lower limits of shear connections are provided for beam applications. In (Couchman, 2015), it is stated that this minimum degree of connection should ensure an elastic behaviour at serviceability limit state and should prevent vertical separation and lateral movement between the concrete layer and the steel part. Out of (EN1994-1-1, 2004) Section 6 (which is valid for beams), the maximum spacing should be 6 times the slab thickness but lower than 800 mm. In (Couchman, 2015), it is however suggested to limit it to 450 mm, the values of (EN1994-1-1, 2004) being recognized as too moderate. On the other hand, in (EN1994-1-1, 2004) Section 9 (which is valid for profiled steel sheeting), a maximum distance of $2h_c$ or 350 mm, whichever is smaller, between the rebar is mentioned. The smaller value of all the above-mentioned prescriptions was respected in the present tests, i.e. $2h_c$ or 300 mm.

As shown in Figure 10, the floor was supported by two supporting systems separated by a distance of 2000 mm. The rotations about the axis of bending were allowed through a roll placed on top of the supports. The overhang length of the specimen at each side was 100 mm (total length 2200 mm). This is the maximum overhang length according to (EN1994-1-1, 2004). It also is prescibed that the width of the bearings should not exceed 100 mm. However, the available supports have a width of 200 mm and 20 mm of thickness. A hinge line can be seen at the center of both supports, due to the elastic bearings pads small horizontal displacement were still possible.

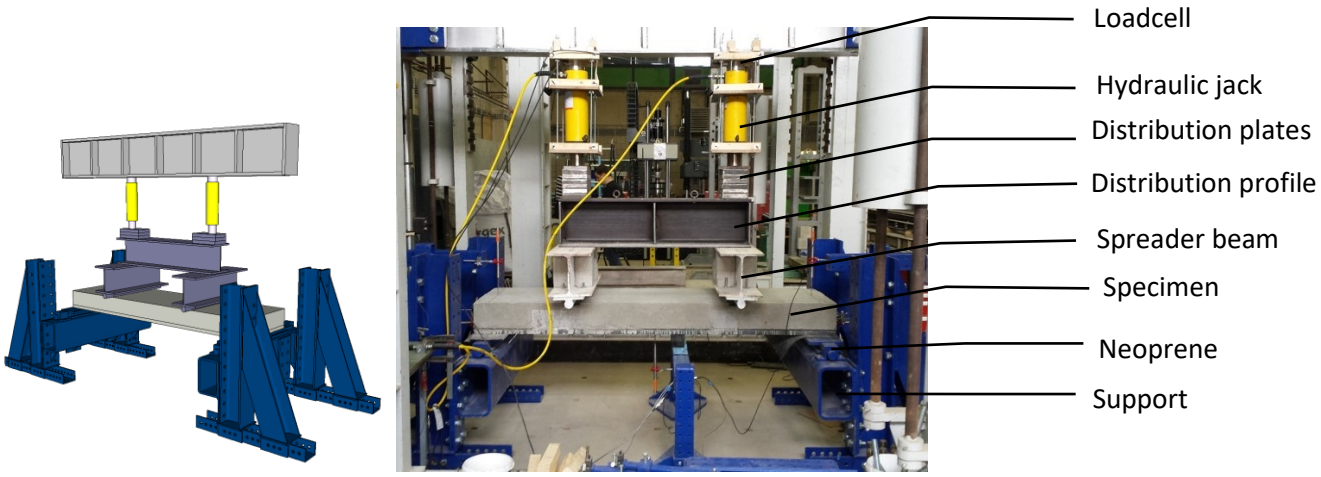

Figure 10: 3D model and test setup in the lab

Two identical line loads were created by using HEB 260 profiles placed on a plain circular section welded to it. The distribution beam was used to hold the spreader beams upright during the test and to evenly distribute the force onto them. The steel plates placed on top of the distribution beam were there to spread the load on it. To eliminate local stresses, neoprene pads were placed in-between the supports and the floor as well as between the loading cylinder and the top surface of the concrete. For the welded specimens, as the bottom surface was not perfectly flat, a layer of high resisting mortar was prepared on top of the supports.

2.2.2 Displacements

In the four-point bending tests, five LVDT's were used to measure the slip, the settlement of the supports and the vertical deflection at mid-span, positioned as displayed in Figure 11 (positions A, B, C, D, E) and Figure 12. A loadcell with a capacity of 800 kN was located on top of each hydraulic jack to measure the correct force at each location.

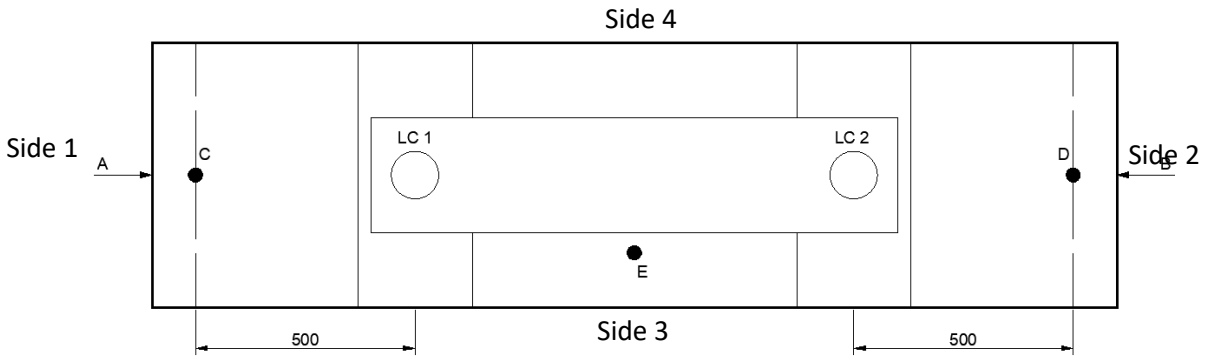

Figure 11: Positioning of the LVDT's

Figure 12: Position and fixation for the relative slip

2.2.3 Testing procedure

The four-point bending tests were carried out according to (EN1994-1-1, 2004) annex B.3. It is also prescribed that 5000 loading cycles between 20% and 60% of the failure load of a specimen tested using a monotonic loading procedure should be done. After this initial phase, the load should be increased so failure does not occur within 1 hour. During our first test, 25 cycles were carried out. It was clear that after one cycle, all chemical bonding was removed and no further influence on the specimen's behaviour was noticed. It was then decided that the load would only be cycled once for the subsequent tests. After this cycle, the load was increased gradually until failure.

3 THEORETICAL CAPACITY

3.1 PUSH-OUT TEST

Assuming that, there is no other connection between the steel and the concrete than the shear connectors themselves, the theoretical maximum capacity of the push-out specimen is given by:

$$P_{max} = n \cdot P_{Rd,stud} \tag{1}$$

where $P_{Rd,stud}$ is the capacity of a single stud and n the amount of studs in the specimen.

The design shear resistance of a stud can be calculated according to EN1994-1-1:2004 using (2) with the smallest value of steel or concrete capacity will be decisive:

$$P_{Rd,stud} = min\left(\frac{0.8 \cdot f_{u,stud} \cdot \frac{\pi \cdot d^2}{4}}{\gamma_v}; \frac{0.29 \cdot \alpha \cdot d^2 \cdot \sqrt{f_{ck} \cdot E_{cm}}}{\gamma_v}\right) \tag{2}$$

where $f_{u,stud}$ is the ultimate tensile strength of the stud, d is the diameter of the shank of the stud, α=1 for the studs used in this study and γ_v is partial safety factor. The maximum theoretical failure load P_{max} for 4 studs thus equals 478,2 kN. Using Oehlers and Johnson's formula (Oehlers & Johnson, 1987), the maximum theoretical failure load would be to 558,0 kN with f_{cu} = 60 MPa and E_{cm} chosen according to EN 1992-1-1. The maximum capacity reached during the test is close to the one predicted by both formulae.

3.2 FOUR-POINT BENDING TEST

3.2.1 Bending capacity

The bending capacity of the system is evaluated considering several options, implementing successively a system with no connection, connection degree equals to or below 1 between the steel and the concrete as well as a cracked or uncracked concrete layer, as illustrated in Figure 13 and Figure 14. These figures are based on the following assumptions; the concrete cannot resist any tensile stresses, the hypotheses that the plane sections before bending remains plane and that the equilibrium of internal stress resultants and connection shear forces shall always be fulfilled.

- Option 1: Assuming that the steel and concrete parts of the specimen are working as a composite member with a rigid shear connection, the strain distribution across the cross-section is linear with no discontinuities (Figure 13(a)) and the maximum capacity reaches 445 kNm. It corresponds to the crushing of the concrete layer. For a moment of 80 kNm – which will turn to be a relevant value for the rest of this study – and a fully composite section, we would reach 128 mm of compressed concrete with a maximum stress of only 15 MPa in the top fibre.
- Option 2: Omitting the composite interaction fully, both parts of the member will slide freely on each other and there is a discontinuity of strains in the connection interface. To ensure that both layers have the same deflection, an equivalent load transferred by each stud is added in the model. In this case, the bending stiffness of the cracked concrete is lower than the one of the steel plate which results in a compressive force to be transferred by each stud (8,7 kN/stud or 31 MPa). Assuming that there is no failure due to shear (in the separate layers), the maximum bending moment that can be attained is 52 kNm (Figure 13(b)) leading to crushing of the concrete and excessive strain in the reinforcement (being considered as 2,5% for a class A rebar). Additionally, a resulting compressive force of 197 kN appears in the concrete layer.

None of these options is consistent with what happened in reality as will be described hereafter. It is nevertheless worth noting at this stage that assuming a compressed area of concrete of 50 mm (Figure 14 (a)), the bending stiffness of both components becomes more or less equal (difference smaller than 10%). The transferred compressive stress increases to 68 MPa, as is the resulting compressive force in the concrete layer (1197kN).

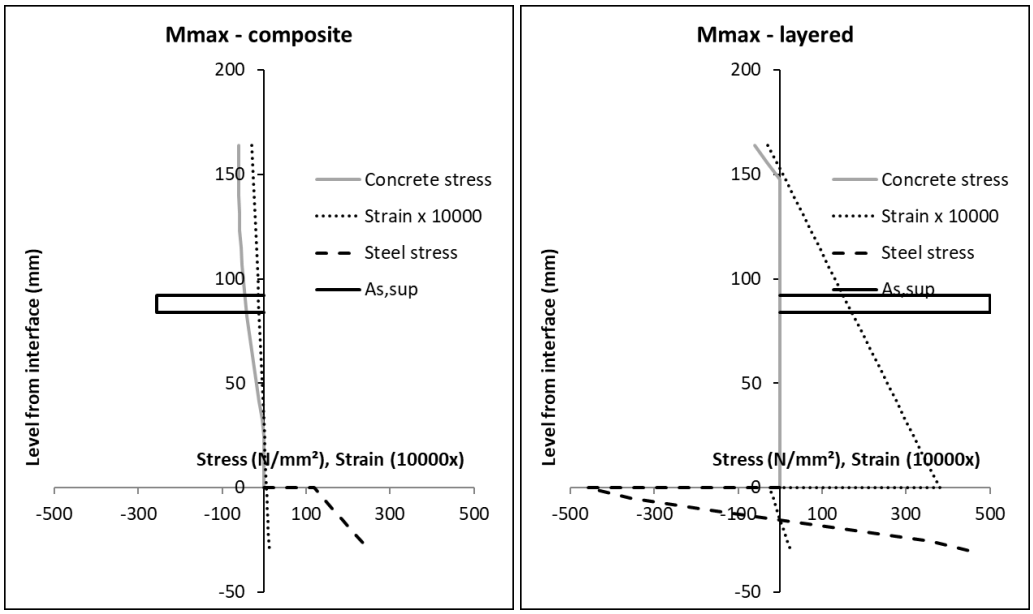

(a) *(b)*

Figure 13: Strain and resulting stress in the cross-section to obtain maximum capacity of the specimen for the options 1 (a) and 2 (b)

- Option 3: In the previous internal equilibriums, the influence of the shear connectors (studs) was neglected. This influence can be introduced as an external force at the location of the steel-concrete interface. This force is working like an external reinforcement for the concrete layer and like a supplementary tensile force in the steel plate. It can be deduced from eq. (2) but activating only 3 studs which correspond to the number of studs present between the extreme sagging and hogging (zero) moments. By doing so, the compressed area increases from 12 (option 2) to 43 mm (based on (EN1994-1-1, 2004)) or even 54 mm (based on (Oehlers & Johnson, 1987)) i.e. depending on the reference used to achieve the calculations. The equilibrium of internal stress resultants and connection shear forces is fulfilled. The bending stiffness of the concrete layer becomes as important as the steel one and the transferred force leads to a tensile stress ranging between 7.4 and 2.1 MPa, according to (EN1994-1-1, 2004) or (Oehlers & Johnson, 1987) respectively. The maximum bending moment capacity would hence be equal to 84 kNm or 80 kNm, according to the expressions provided in (EN1994-1-1, 2004) or (Oehlers & Johnson, 1987) respectively.

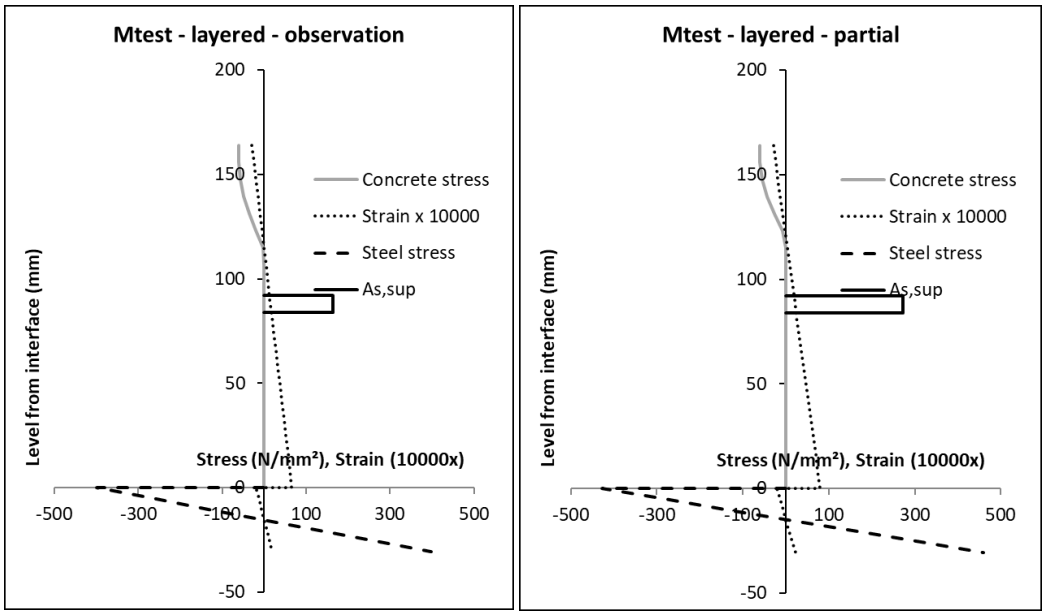

(a) *(b)*

Figure 14: Strain and resulting stress in the cross-section based on observations during the tests (a) and for the option 3 according to EC4-1-1 (b)

It is worth mentioning that the concrete layer will be even stiffer due to the (small) tensile capacity of the concrete. Hence an arch effect can develop leading to wider uncracked area in the concrete. It could therefore happen that the concrete layer would become stiffer than the steel plate, causing an even higher transferred tensile stress, as mentioned in option 3.

3.2.2 Bending stiffness

Besides the failure load, it is also desirable to predict the behaviour of the specimen during loading. It is clear that a different stiffness will be obtained depending on the degree of longitudinal shear connection. Presently, due to the low degree of shear connection, the system is not a solid composite section, but a partial connection should be considered. In the worst-case scenario, we could consider that the two layers work as stacked layers (labelled "layered" later on) without interaction. It is important to estimate the height of the uncracked concrete area, with *z* the position of the gravity centre of the section, *x* the height of the uncracked concrete and, the bending stiffness will be equal to:

$$(E \cdot I)_{composite} = E_{cm}\left(\frac{bx^3}{12} + bx\left(z - \frac{x}{2}\right)^2\right) + E_s A_s (z - (h_c - a))^2 + E_a\left(\frac{bt^3}{12} + bt\left(\left(h_c + \frac{t}{2}\right) - z\right)^2\right) \quad (3)$$

In Figure 15, depicting the bending stiffness for the cases previously mentioned, it is highlighted that the degree of cracked concrete area strongly influences the bending stiffness. It can be seen that, with a very small compressed concrete area, a cracked composite section reacts as uncracked stacked layers.

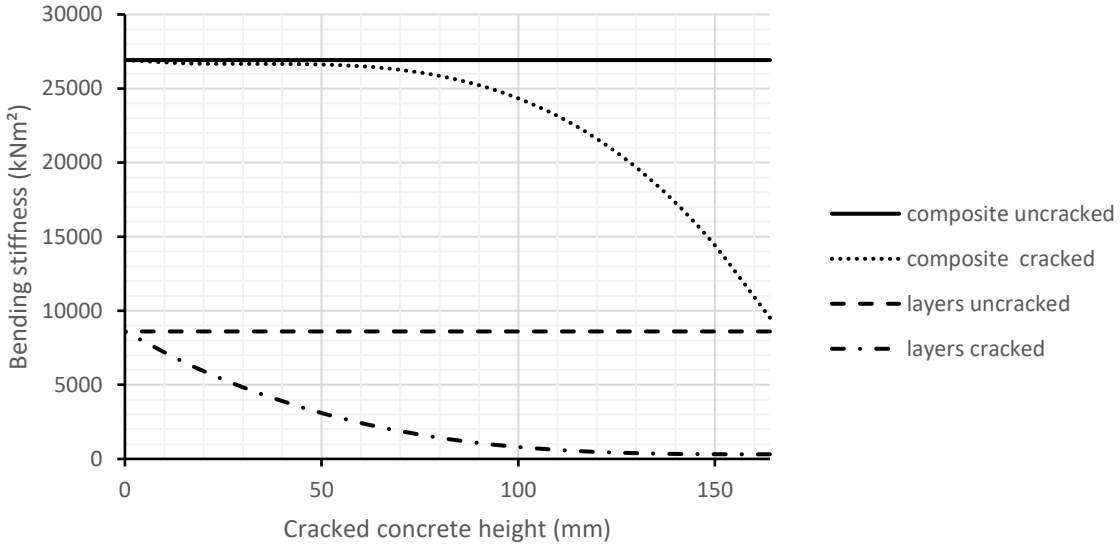

Figure 15: Bending stiffness depending of cracked concrete height

Table 3: Stiffnesses of components, composite and layered element

Component	**Bending stiffness EI uncracked** [kNm²]	**Bending stiffness EI cracked** [kNm²] *x* = 50 mm
Concrete	8292	235
Rebar	0,04	0,04
Steel plate	312	312
Composite	26920	22579
Layered	8604	547

The height of the uncracked area can be evaluated by means of Bernoulli's law, depending on the moment, hence it varies along the length of the element. This is only possible as long as we are working in the elastic domain and perfect contact (without slip) can be guaranteed, which makes it difficult for low connections grades. A good approximation can be found by introducing for *x* the height of the concrete above the head of the stud. In our experiments, the thickness of concrete above the crack initiator equals 50mm. *Table* 3 provides the different stiffness values with x = 50 mm as uncracked concrete height (or, based on Table 2, considering about 164 – 50 =114 mm of cracked concrete).

3.2.3 Load-deformation relation

By neglecting the effect of the dead load of the slab itself, the deflection of an element can be described by the following equation based on structural mechanics:

$$\Delta = P \cdot \frac{L^2 a}{24(EI)_{element}} \left(3 - 4 \cdot \left(\frac{a}{L}\right)^2\right) \tag{4}$$

Taking into account the dimensions of Figure 16, this can be worked out for different values of $(EI)_{element}$ (as composite or layered). The outcome of that equation will be depicted in the figures of chapter 5.

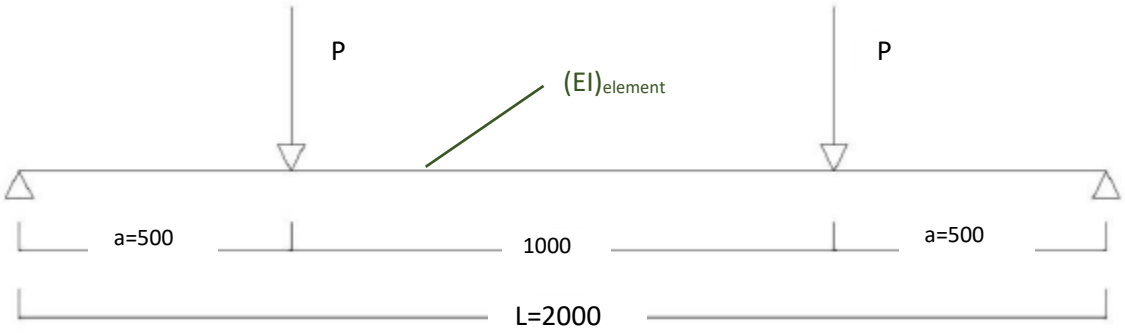

Figure 16: Principal schema of the executed four-point bending test

3.2.4 Shear failure (vertical shear)

Bending failure will occur if the shear capacity of the composite section is sufficiently high to avoid shear failure. Typically, this is guaranteed by the stiffest element in the system.

For a composite beam, with a rather high bending stiffness of the steel beam compared to that of the concrete layer, the vertical shear capacity is determined by the capacity of the web unless an evaluation of the concrete contribution can be made.

In the actual experimental programme, with a thickness of 164 mm of concrete on top of a 31 mm steel plate, none of the above simplifications is valid. Vertical shear forces are distributed between the different elements in proportion to their contribution to the bending stiffness of the system. The most unfavourable situation is obtained in the case of layered components with cracked concrete. It can be seen that the concrete contribution in such case will be equal to 235/547 = 43% of the total shear force. Calculating the maximum concrete shear capacity and dividing it by the previous ratio will provide the maximum shear capacity.

Following (EN 1992-1-1, 2004), the concrete shear capacity is given by:

$$V_{Rd,c} = MAX(C_{Rd,c}k(100\rho_l f_{ck})^{1/3}\,;0.035.k^{2/3}f_{ck}^{1/2})b\cdot d_{\text{conc}} \qquad (5)$$

where $k = (1+\sqrt{(200/d_{conc})})=2{,}83$ & <2, $\rho_l = A_s/(b\cdot d_{conc}) = 0{,}0056$, d_{conc} is, in this case, equal to the distance from the top of the concrete to the centroid of the reinforcement bars i.e. 60 mm and f_{ck} = 60 MPa. Presently, a value of 41,8 kN is obtained. It is equal to 43 % of the total shear capacity, hence the latter equals 97,2 kN. To obtain the maximum actuator load, a small correction V_{DL} is needed to take into account the dead load of the slab itself, the 2 HEB260 profiles, the distribution beam (HEB300) and the distribution plates. In total, a maximum value of 90,7 kN is found.

Another approach can be contemplated in which the concrete deck is considered as an unreinforced layer. In this case, k=2,1 or 2, $\rho_l = 0$ and $d_{conc} = h_c$. Therefore, $V_{Rd,c}$ equals 42,3 kN, leading to an actuator load of 92,0 kN. Both values are very close to each other.

Of course, the shear capacity of the steel plate is much higher than the one of the concrete layer but the steel plate considered alone can only sustain 66.2kNm in bending if fully plastic (44,1 kNm if elastic).

4 PUSH-OUT TEST - RESULTS AND DISCUSSION

4.1 TEST RESULTS FOR PO-NW

The load-slip graphs for PO-NW are shown in Figure 17. During the performed loading cycles, the slip of LVDT 2 gradually increased then impaired indicating that the chemical bond between the steel and the concrete was broken. At the level of the three other LVDT's there was no significant increase of the slip during the cycles. The graphs of LVDT's 3 and 4, positioned on the same side, were very consistent.

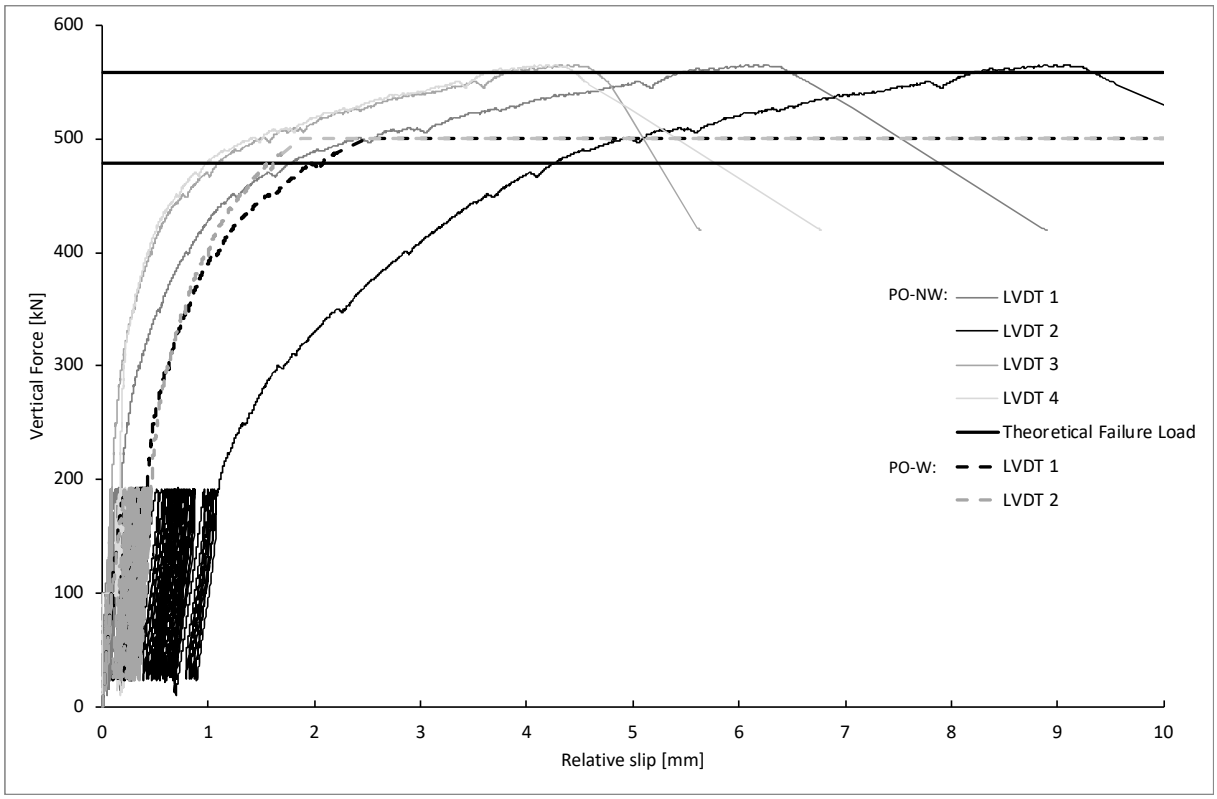

Figure 17: Load-slip comparison

No cracks on the outside surface of the concrete slab occurred during loading. At a maximum load of 565,12 kN, the studs in the slab underneath LVDT's 1 and 2 failed in shear. Note that the maximum value according to Oehlers and Johnson's formula (Oehlers & Johnson, 1987) for 1 stud equals 139,5kN.

Based on Figure 17, it can be seen that the characteristic slip capacity δ_{uk} as defined in (EN1994-1-1, 2004) annex B is higher than 6 mm, which is the boundary for ductile behaviour. Only one measured slip (LVDT 3) appears to be less. However, looking to its position on Figure 6, the mean value of both LVDT1 and 3 should be considered which is above the previously mentioned minimum value of 6 mm.

The stud was removed from the concrete and prepared for microstructure analysis. The failed stud originating from PO-NW-were cut using a wire-EDM as illustrated in Figure 18 (right). During removal, it was noticed that the concrete around the stud was cracked allowing the stud to deform substantially before fracture. Figure 18 (left) shows one other stud after the concrete was removed. It is clear that a large plastic deformation had already taken place when the studs on the other side failed.

Figure 18: Plastic deformation of the stud (left) and cutting the sample using a wire-EDM (right)

The use of a microscope gives a general indication of the different zones present around the weld, Figure 19. It could be noticed that the shear stud failed in the base metal near but outside the heat affected zone and that failure started in the heat affected zone (on the right side of the specimen). In Figure 20, one can notice that fracture extended through the stud from the heat affected zone producing a smooth fracture surface.

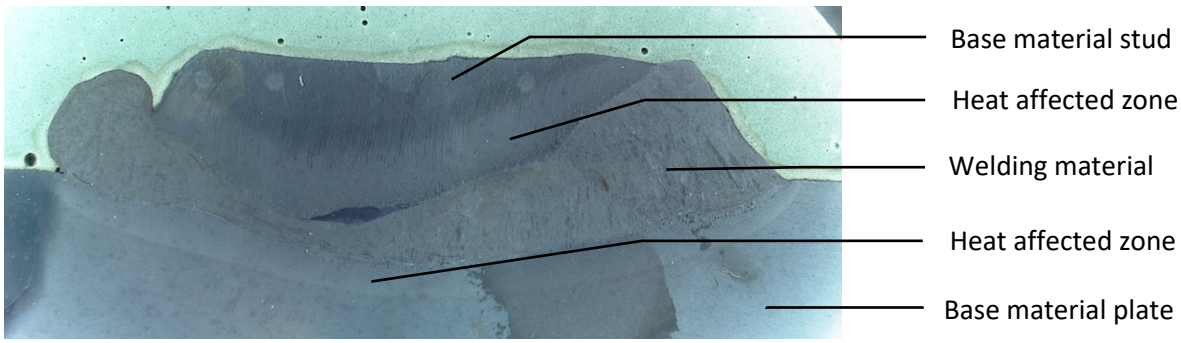

Figure 19: Macroscopic image of the weld

Figure 20: Fracture surface of PO-NW (left) and PL-1 (right)

4.2 TEST RESULTS FOR PO-W

The load-slip graphs for PO-W are shown in Figure 17. Unfortunately, the measurements taken by LVDT 3 and LVDT 4 stopped in the beginning of the testing procedure. This means that the available slip values are all from the same side. The 25 loading cycles can clearly be seen on the graphs. During these cycles, the slip gradually increased then stabilized only after a few cycles, due to the chemical bond between the steel and the concrete being broken. The load-slip curves have similar shapes for all specimens.

At a load of 488 kN, it was deemed too dangerous to keep the LVDT's in place therefore the ultimate load cannot be seen on the graph. Nevertheless, in Figure 17, the horizontal line shows when failure occurred at a maximum load of 500,63 kN. In this case, the concrete failed by splitting. After the test, it was removed to inspect the state of the studs which were plastically deformation due to shear (Figure 18) although still far from fracture.

4.3 COMPARISON OF BOTH SPECIMENS

The stiffness, the general course of the graphs and maximum loads are very similar for both tests, with the exception of LVDT 2 in PO-NW-2.

A summary of the test results of PO-NW and PO-W is provided in Table 4.

Table 4: PO-NW-2 and PO-W-1, push-out tests

	f_{ck}		$P_{f,total}$	P_{rk}	δ_u		δ_{uk}	
	[N/mm²]		[kN]	[kN]	[mm]		[mm]	
	Side 1	*Side 2*			*Side 1*	*Side 2*	*Side 1*	*Side 2*
PO-NW-2	75,63	77,86	565,12	127,15	5,48	4,39	1,35	0,95
PO-W-1	74,87	66,65	500,63**	112,64**	*	*	2,00	1,58

**LVDT's were removed before failure*

***Concrete failure*

The maximum capacity reached during the test is close to the one predicted by (EN1994-1-1, 2004) (which was 478,2 kN for 4 studs) or based on Oehlers and Johnson's formula (Oehlers & Johnson, 1987) (leading to 558,0 kN). Although there is an 11,5% difference between the failure load of PO-NW and PO-W, in practice, no difference was noticed between the behaviour of shear studs welded on a weld compared to shear studs welded on the steel plate. When the concrete failed in PO-W, the studs had not yet reached their full plastic deformation capacity. The behaviour of both specimens was very similar. One could claim that reinforcement could have prevented that premature failure although, as described in (Oehlers, 1989), transverse reinforcement does not prevent splitting, but the splitting is limited and therefore the loss of interaction of the shear connection is also limited. Therefore, based on these tests, it can be concluded that the shear capacity of a shear stud is unaffected when this stud is welded on a butt weld.

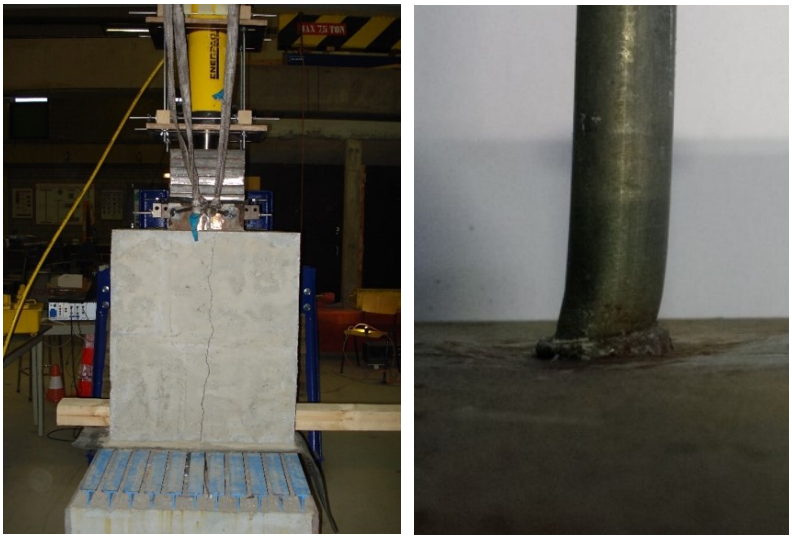

Figure 21: Failure of the specimen

5 FOUR-POINT BENDING TESTS- RESULTS AND DISCUSSION

In this chapter the test results of the four-point bending tests on floors will be discussed and compared. The displacements measured at the positions C and D, Figure 11, could enable to correct the vertical displacements obtained in the middle of the beam by the settlements of the supports.

5.1 TEST RESULTS FOR PL-2 AND 3

Figure 11 helps understanding the different sides of the floor. Side 1 and 2 are situated in the transverse direction of the specimen. Side 3 and 4 are located in the longitudinal direction of the specimen. Figure 22 and Figure 23 respectively shows the load-displacement and the load-slip graph for the test on specimens PL-2 and PL-3. The first specimen could not be tested. Points #1 and #3 are characterized by the sudden breaking of the chemical bond on side 2 and 1 respectively between the steel and the concrete. The slip visibly starts to increase at points #1 and #5, an opening was present. On point #4, a vertical crack at side 1 was clearly visible and expanded up to point #6. Point #2 shows the starting of the concrete cracking in bending, see Figure 24. Point #7 corresponds to the audible failure of the studs.

For both tests, besides a shift due to the loss of chemical bound and subsequent slip, the experimental initial stiffness was in good agreement with the calculated theoretical one of a floor without considering any connection between the concrete and the steel i.e. stacked separate layers with uncracked concrete. While the chemical bond is already lost in the beginning of the test, the influence of the cracking of the concrete becomes significant around 90 kN. This can be noticed in Figure 22 as the slope of the experimental load-deflection diagram is then in good agreement with the one of stacked layers and cracked concrete (considering 50 mm of uncracked concrete based on our visual observations). The loss of the chemical bond is also visible on Figure 23 for PL-2 as there is a sudden increase of the slip at both sides of the specimen. Towards the end of the test, the load-deflection slope becomes parallel to the theoretical one considering a system with no connection as the previous one and with cracked concrete. The LVDT's were prematurely removed to ensure the safety of the measuring equipment. The specimens failed in the concrete at an ultimate load of 155,6kN and 146,2kN for PL-2 and PL-3 respectively. After the test, the concrete was removed from the specimens and it was established that the shear studs were also ruptured.

As mentioned above, the conversion from a system with uncracked concrete to one with cracked concrete takes place around 90 kN. This value is also equal to the shear capacity of the upper reinforced layer (90,7 kN), or the capacity of the unreinforced concrete (92 kN) as indicated in 3.2.4. However, during the test, shear cracks are only developing from the point of interest #6 in Figure 22. As for flexural cracks, they are already present as from point #2, and, it was shown in Figure 14 that the second moment of area rapidly decreases at that moment. Besides, it happens to be around 90 kN too that the steel plate starts to yield. Considering its fully plastic capacity, the plate can only withstand 132 kN (i.e. for a moment of 66.2kNm) while the concrete layer could add at the maximum only 11 kN to it. In fact, after the test, some permanent deflection could be observed (as indicated in Table 5). Therefore, it becomes clear that another mechanism took place during the test and enabled the system to reach its maximum capacity. The obtained high bending capacity of the system can only be explained by compressive membrane action in the concrete suspending the steel plate on a concrete arch. The studs, playing a crucial role at that moment, are not only loaded in shear but also in tension, which can explain the surface roughness seen in Figure 20.

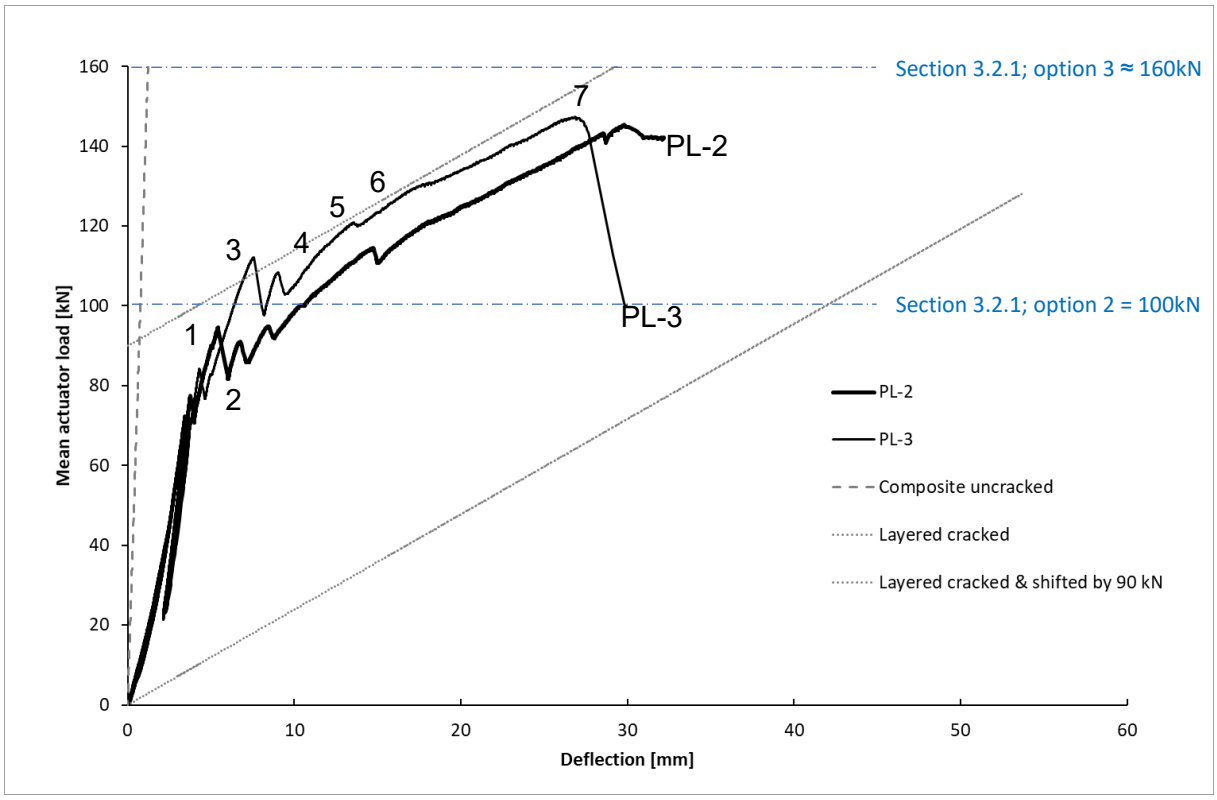

Figure 22: Load-displacement PL-2 and 3 with points of interest

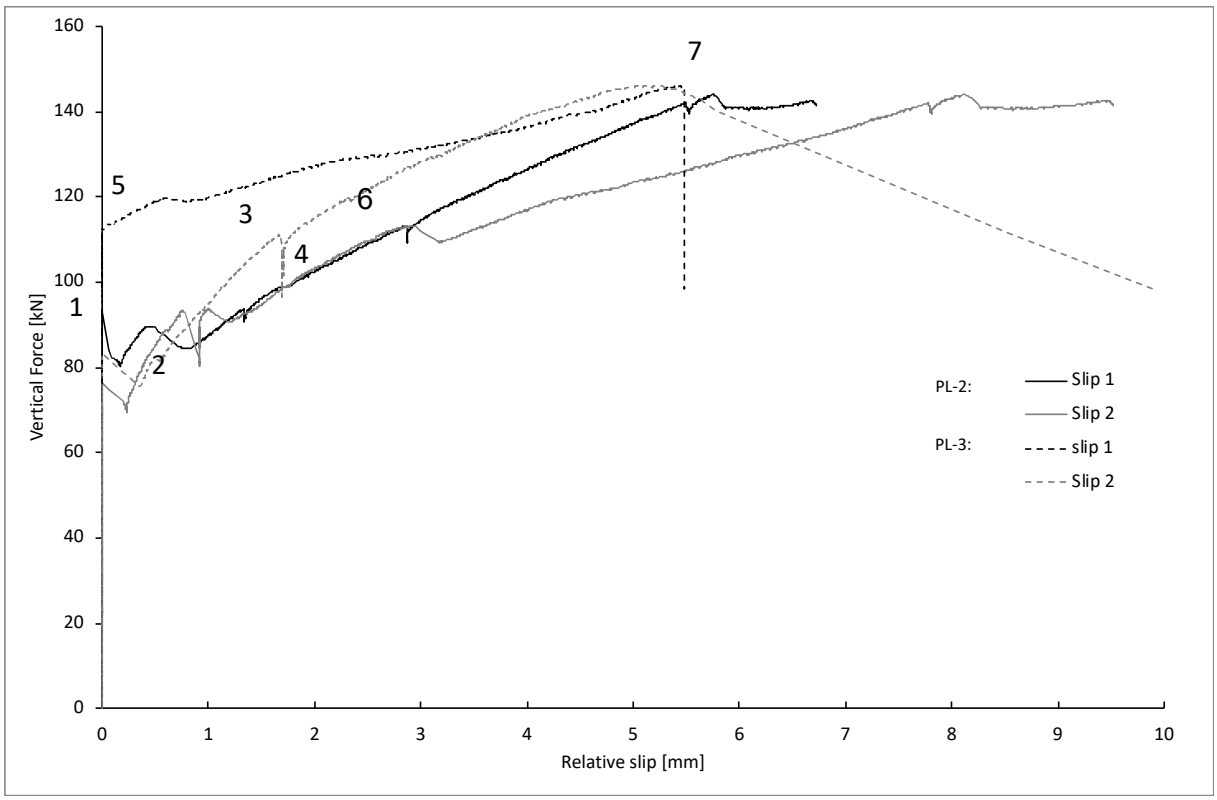

Figure 23: Load-slip PL-2 and PL-3 Load-slip PL-3 with points of interest

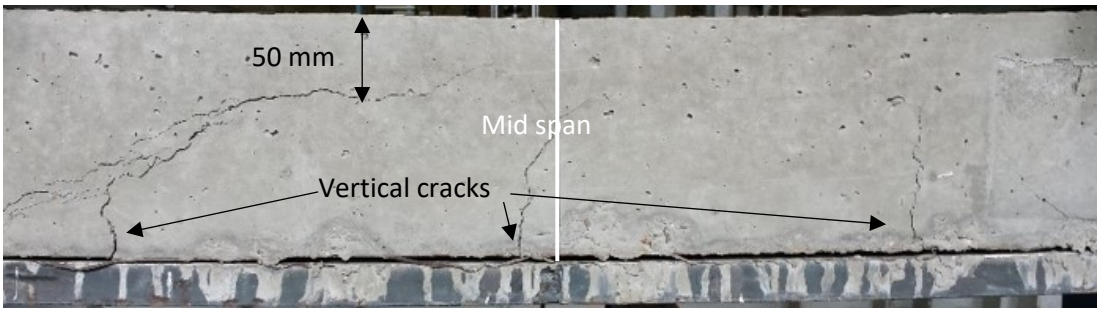

Figure 24: Development of cracks during test

It was noticed that even with shear connectors placed at 300 mm depth, from the side surface of the test specimen, they seems to work as crack initiators. Comparing Figure 24 with the position of the shear studs, Figure 9, makes this clear. Where the shear studs are meant to enhance the capacity of a cross section by activating composite action, it can also lead to cracked concrete for comparable situations as the one tested. This underlines that the consequences of this local phenomenon to the global analysis should be verified.

5.2 TEST RESULTS FOR WE-1, 2 AND 3

During those tests as well, the LVDT's were prematurely removed for safety reasons. An audible failure of the shear studs was also noticed for WE-1. The studs sheared off at a maximum load of 155,0kN. For WE-2 and 3, the specimen failed in the concrete (excessive strains) at a force of 165,8kN and 155,6kN respectively. When the setup was relaxed, there was an audible shear stud failing.

In WE-3, points #1 and #2 are characterized by a vertical crack at side 1 and then 2 with a corresponding jump of the slip. At points #3 and #4, the flexure cracking is fully developed across the concrete beam. For all three tests, the initial stiffness is in good agreement with the calculated value, both at an initial stage as well as when the chemical bond is totally broken.

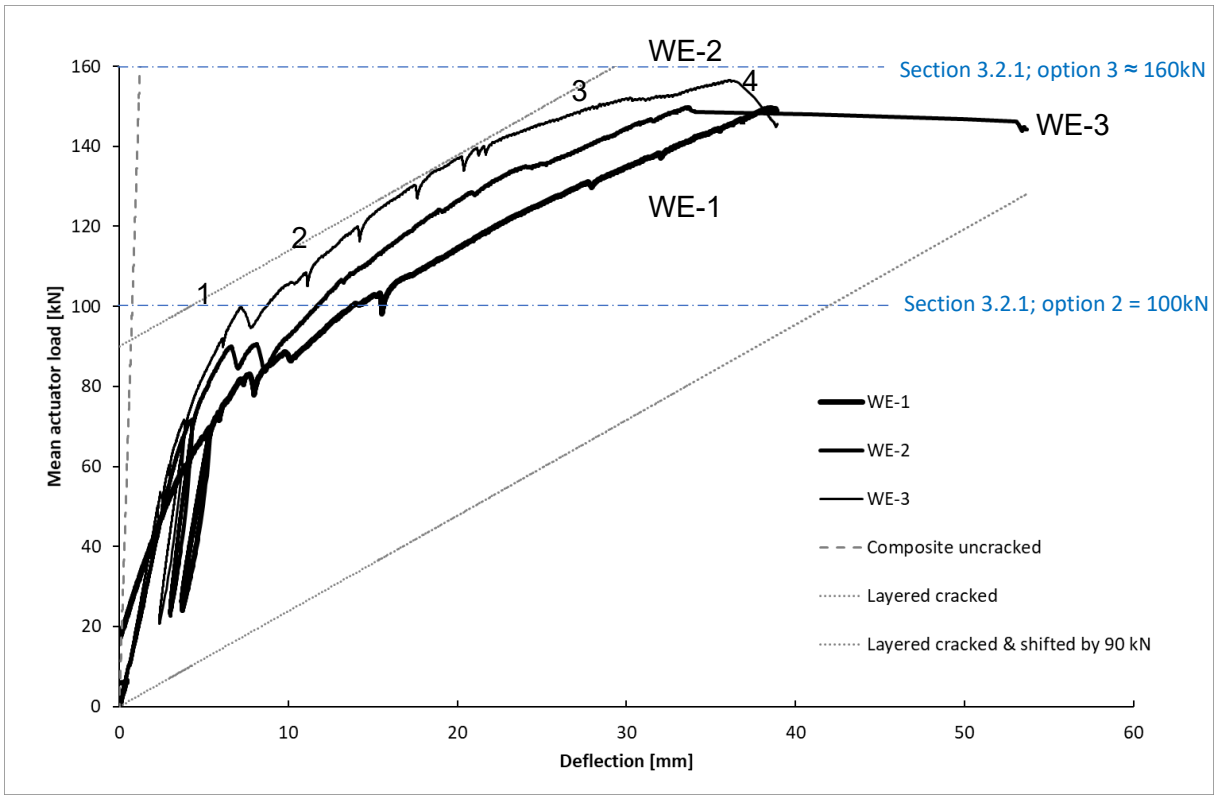

Figure 25: Comparison of the welded specimens (WE-2 with points of interest)

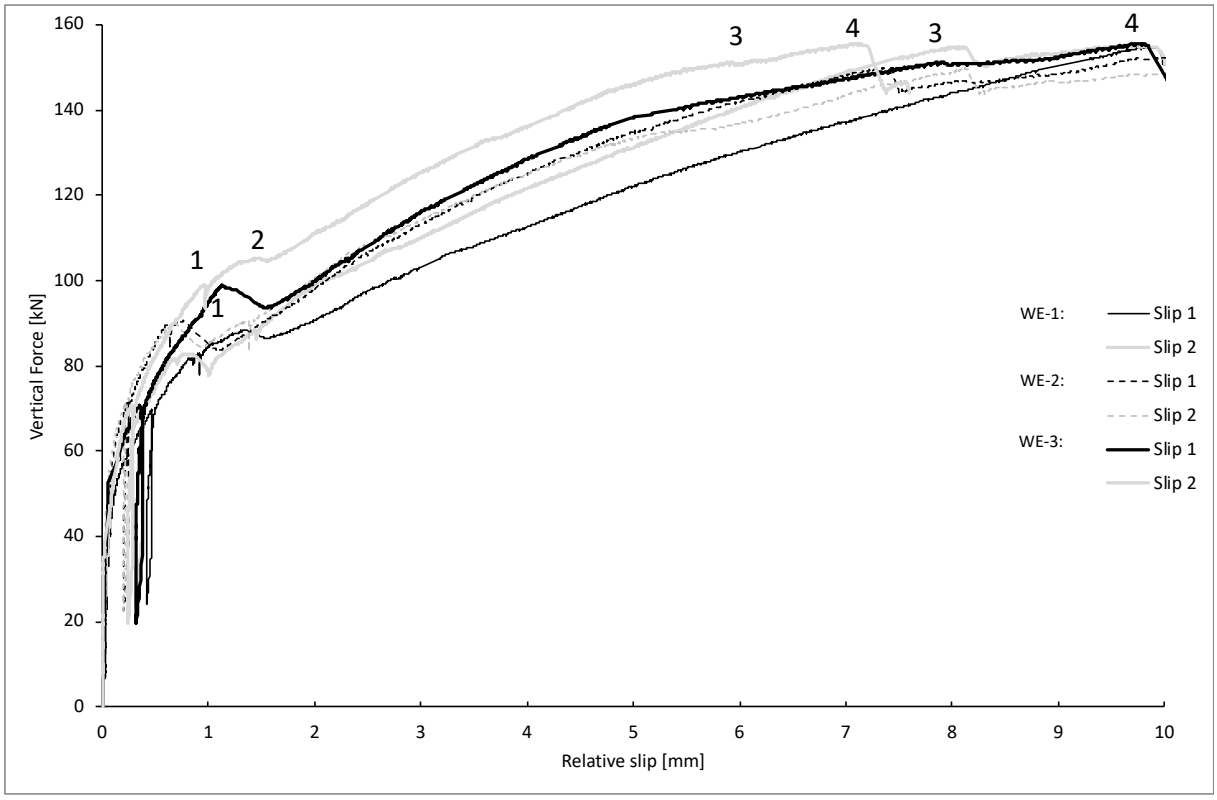

Figure 26: Load-slip WE-3 with points of interest

5.3 COMPARISON OF BOTH SPECIMENS

Table 5 gives an overview of the different results for each specimen.

Table 5: Comparison of welded and non-welded beam specimens

	PL-2	PL-3	WE-1	WE-2	WE-3
Maximum load [kN]	155,56	146,16	155,04	165,76	155,64
Chemical bond lost [kN]	±90	±80	±80	±90	±80
Failure mode	Concrete	Stud	Stud	Concrete	Concrete
Residual deformation [mm]	5,5	10	14	11	13

The maximum load for each specimen is 150,9kN and 158,8kN for the non-welded and welded specimens respectively. The initial stiffness of the welded specimens is slightly lower than the stiffness of the specimens without a weld. It is possible to evaluate the theoretical loss of stiffness of a steel plate when there is a weld present in its middle. When this is taken into consideration, no significant differences can be observed between the behaviour of the specimens with a weld and the specimens without a weld. Therefore, it is concluded that the shear capacity of a shear stud is unaffected when this stud is welded on a butt weld.

6 CONCLUSIONS

The purpose of this research was to investigate the effect of welding a line of headed shear studs on top of a butt weld on the global shear resistance of a composite system. Two types of tests were carried out based on (EN1994-1-1, 2004). A push-out test was performed to evaluate the connection in pure shear. The four-point bending tests had the purpose to evaluate the shear studs in a way they would normally be used in practice.

During the push-out tests, the specimens behaved as expected. The push-out tests showed that the maximum failure load is in very good agreement with the calculated theoretical one, according to (EN1994-1-1, 2004) or to the Oehlers-Johnson's equation, the latter delivers the best approximation of the ultimate load.

During the four-point bending tests, the ultimate behaviour of the system combined the flexural resistance of a composite cross-section followed by, when the concrete is cracked, the development of a compressed arch anchored in the headed shear studs. The bending capacity of the system was then evaluated considering several options, implementing successively a system with no connection, connection degree equal to or below 1 between the steel and the concrete as well as a cracked or uncracked concrete layer. Based on the visual observations during the test and on the measurements, the best option was discussed.

The bending stiffness of the system, also considering successively a cracked or uncracked concrete layer with a varying degree of connection with the steel plate, was also calculated and put into relation with the experimental stiffness and its evolution during the test.

Based on the ultimate load obtained experimentally during the four-point bending tests, it is then demonstrated that a failure mechanism involving the development of an arch in compression working with the steel plate in tension is taking place. The development of such a failure mechanism would not be possible without the presence of the headed shear studs. The measured failure loads fit very well the ones mentioned in the theoretical section based on that assumption.

In conclusion, no significant differences in the behaviour of both specimens (with a butt weld or not) were observed. In both cases, the shear stud failed in its own shaft meaning that the connection to the steel is not compromised by the presence of a butt weld.

References

Alkhatib, A., 2012. *Experimental study of behaviour and strength of shear studs in composite bridge deck construction.* Halifax, Canada: Dalhouse University.

An, L. & Cederwall, K., 1996. Push-out Tests on Studs in High Strength and Normal Strength Concrete. *J. Constr. Steel Res.,* Issue 36, pp. 15-29.

Anon., 2012. *Testing hardened concrete - Part 1 : Shape, dimensions and other requirements for specimens and moulds.* Brussels: European Committee for Standardization.

Anon., n.d. *http://studmaster.co.in/all-products/welding-machines/consumables-accessories/shear-connectors.* [Online].

Cashell, K. A. & Baddoo, N., 2013. *Experimental assessment of ferritic stainless steel.* North Queensland, Australia, s.n.

Couchman, G., 2015. *Minimum degree of shear connection rules for UK construction to Eurocode 4.* Berkshire, UK: The Steel Construction Institute.

Easterling, W. S., Gibbings, D. R. & Murray, T. M., 1993. Strength of shear studs in steel deck on composite beams and joists. *Engineering Journal,* Issue 30, pp. 44-54.

EN 1992-1-1, 2004. *Eurocode 2: Design of concrete structures - Part 1-1: General rules and rules for buildings.* Brussels: CEN.

EN1994-1-1, 2004. *Eurocode 4: Design of composite steel and concrete structures - Part 1-1: General rules and rules for buildings.* Brussels: CEN.

Horita, Y., Tagawa, Y. & Asada, H., 2012. *Push-out test of headed stud in composite girder using steel deck -An effect of stud length of projecting part from steel deck on shear strength.* Lisbon, Portugal, s.n.

Kumar, P., Chaudhary, S. & Gupta, R., 2017. Behaviour of adhesive bonded and mechanically connected steel- concrete composite under impact loading. *Procedia Engineering,* Issue 173, pp. 447-454.

Lowe, D., Das, R. & Clifton, C., 2014. Characterization of the splitting behavior of steel-concrete composite beams with shear stud connection. *Procedia Material Science,* Issue 3, pp. 2174-2179.

Oehlers, D., 1989. Splitting Induced by Shear Connectors in Composite Beams. *Journal of structural engineering,* Issue 15.

Oehlers, D. & Johnson, R., 1987. The strength of stud shear connections in composite beams. *The Structural Engineer,* Issue 65, pp. 44-58.

Prakash, A., Anandavalli, N., Madheswaran, C. K. & Lakshmanan, N., 2012. Modified Push-out Tests for Determining Shear Strength and Stiffness of HSS Stud Connector-Experimental Study. *Int. J. Composite Materials,* Issue 2, pp. 22-31.

Qi, J., Wang, J., Li, M. & Chen, L., 2017. Shear capacity of stud shear connectors with initial damage : Experiment , FEM model and theoretical formulation Shear capacity of stud shear connectors with initial damage : Experiment , FEM model and theoretical form. *Steel and composite structures,* Issue 25, pp. 79-92.

Rehman, N., Lam, D. & Dai, X. A., 2018. Testing of composite beam with demountable shear connectors. In: *Proceedings of the institution of Civil Engineers - Structures and Bridges.* s.l.:ICE Publishing, pp. 3-16.

Shim, H., Park, S. & Lee, J., 2010. *Push-out tests on shear studs in high strength concrete.* Seogwipo, Korea, s.n.

standardization, E. c. f., 2004. *Eurocode 2: Design of concrete structures - Part 1-1 General rules and rules for buildings.* Brussels: CEN.

Wang, Q., Liu, Y. & Luo, J., 2011. *Experimental Study on Stud Shear Connectors with Large Diameter and High Strength.* Lushan, China, s.n.